Proceedings of the ASME 2010 3rd Joint US-European Fluids Engineering Summer Meeting and 8th International Conference on Nanochannels, Microchannels, and Minichannels
FEDSM-ICNMM2010
August 1-5, 2010, Montreal, Canada

FEDSM-ICNMM2010-31060

A Numerical Model on Secondary Flow and Mixing in Rotating Microfluidics

Wallace Woon-Fong Leung*[1,2] and Yong Ren[2]
[1] Research Institute of Innovative Products & Technologies
[2] Department of Mechanical Engineering
The Hong Kong Polytechnic University, Hung Hom, Kowloon, Hong Kong

*Corresponding Author and presenter.

Abstract

The fluid mechanics of mixing different species in a closed rotating microfluidics chamber was investigated. Complicated secondary flow, in form of vortices, in a rotating chamber was generated for mixing different species by continuous changing the rate of rotation over time until uniform mixing of the different species in the chamber has been attained. Three vortices are observed when reference to the rotating chamber – one main vortex in the R-θ planes, generated from the d'Alembert force, was responsible for momentum and mass transfer while two pairs of toroidal vortices, generated from the Coriolis force, is responsible for momentum and mass transfer in the direction parallel to the rotational axis. These secondary flow and vortices help to reduce the mixing length between species of a given concentration. With a much smaller mixing length, diffusion can further effect the remaining mixing in a more reasonable time for the mixture to attain a more uniform or homogenous condition of the species in the microfluidic chamber.

Numerical simulation using ANSYS-CFX was used to solve the transient Navier-Stokes equation in the rotating frame simulating the Newtonian laminar flow pattern for linear acceleration and deceleration (in rotation) schemes. Mass transfer was also modeled using the convective-diffusion equation governing movement of the different species in the chamber after the NS and continuity equations have been solved for the velocity field. Using the numerical model, parametric study of the rotating truncated pie-shaped chamber (radius and angular span) have been carried out to investigate the effect of momentum and mass transfer. An index, the mixing quality based on concentration distribution for the whole domain, was used respectively to quantitatively evaluate the mixing performance.

Background

Passive mixing [1-11] in microfluidics has been studied extensively by many researchers as it does not involve direct mixing of external mixing elements with the small liquid sample in microfluidics, which is an attractive advantage. One effective passive mixing in microfluidics is by rotating the chamber in form of a CD, see Fig. 1. Rotating microfluidics is rather new and only recently studied. Almost all the literature on this new topic focuses around the applications [12-24]. For mixing, one can perceive that the disk and chamber contained therein is rotated in one direction (say clockwise/anticlockwise) and subsequently rotated in the opposite direction (say anticlockwise/clockwise) [12]. This generates a sloshing motion for mixing as in common practice of mixing of coffee in a cup during driving. However, the fluid mechanics of the flow as a result of such sloshing motion is not understood, therefore the result on mixing of different liquids and species dissolved/suspended in the liquids using rotating microfluidic can only be used, at best, on an ad-hoc basis. A numerical model for fluid flow in an enclosed rotating chamber is developed in this study. Further, assuming different species (small dissolved or suspended solids) are present in the liquid or liquids, we study mixing of these species due to the fluid motion generated from sloshing – in a more scientific term, under the influence of inertial forces arising from acceleration and deceleration of the chamber. The intent of this study is to fill the missing gap in understanding of the fundamental of fluid flow and mixing in rotating microfluidic.

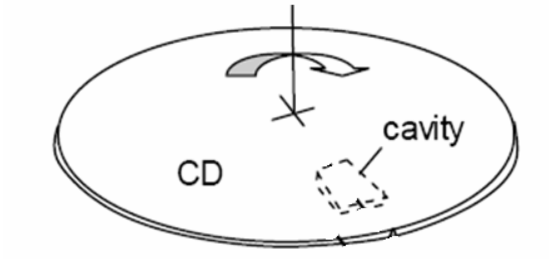

Fig. 1 – Cavity or chamber in a rotating CD.

Numerical Model

Mixing after-all takes place at two levels. On a macro level, we rotate the chamber in such a manner that we reduce the mixing distance or mixing length of a given species. Once this state is reached, molecular diffusion (or random walk) of the species takes over and getting species mixed effectively in a much smaller mixing length. Next, we investigate the macro level of reducing the mixing length by using secondary flow generated in both the R-θ planes and the R-z planes, as a result of inertial acceleration/deceleration of the chamber.

The unsteady-state incompressible flow in a rotating microfluidic chamber is governed, respectively, by the continuity equation,

$$\nabla \cdot \vec{q} = 0 \tag{1}$$

For incompressible flow, the radial, tangential, and axial velocity components in Eq. 1 have to satisfy the continuity equation or mass conservation in that there is no net mass leaving a control volume.

In addition, the velocity components respectively along the radial, tangential and axial directions should conform to the Navier-Stokes equation,

Fluid acceleration in rotating frame

Force/Mass in rotating frame

$$\frac{D\vec{q}}{Dt} = -\frac{\nabla P}{\rho} + \nu \nabla^2 \vec{q} - \vec{\Omega} \times (\vec{\Omega} \times \vec{r}) - 2\vec{\Omega} \times \vec{q} + \vec{r} \times \frac{d\vec{\Omega}}{dt} \tag{2}$$

Pressure Gradient — Viscous term — Centrifugal term — Coriolis term — D'Alembert term

For the right side of Eq. 2, the first term represents the pressure gradient, second term the viscous resistance force, third term the centrifugal acceleration (always radial outward), fourth term the Coriolis acceleration due to relative velocity in rotating reference frame, and fifth term the d'Alembert acceleration due to acceleration of the microfluidic chamber. These accelerations or forces per unit mass affect the ultimate acceleration/deceleration of a fluid particle in time and space as observed in the rotating reference frame (left side of Eq. 2).

These 4-scalar nonlinear equations are solved using ANSYS-CFX software in a rotating reference frame for the truncated chamber as shown in Fig. 2. The geometry of the rotating chamber is determined by the outer radius R_o, inner radius R_i, span angle θ, and the half height of the chamber H.

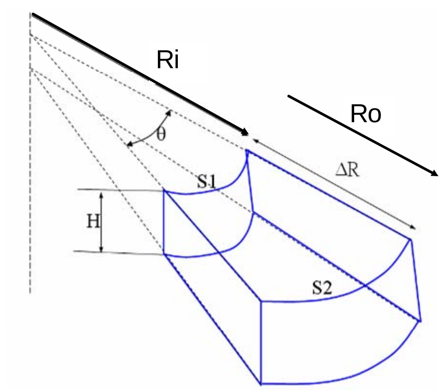

Fig. 2 – Pie-shaped microfluidic chamber being studied.

As shown in Fig. 3, the chamber is meshed with both structured hexahedral elements in the core region and unstructured prismatic elements especially near the walls where boundary layers are present.

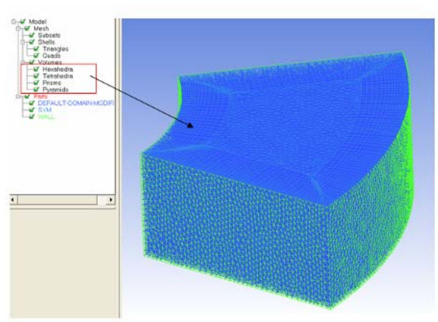

Fig. 3 – Meshing of microfluidic chamber.

The chamber is being linearly accelerated over time to a maximum value and subsequently linearly decelerated to zero speed (halt). This forms one complete cycle and the cycle is repeated thereafter.

By way of example, we illustrate below the result of a simulation wherein the chamber is accelerated in rotation in one sense (say counterclockwise) from 0 to 160 rad/s linearly from rest to 0.5 s, and subsequently decelerated linearly over time to rest in the following 0.5 s. The total cycle time is 1 s, and this cycle is repeated. The rotation sense is always kept the same [26] (say either clockwise or anticlockwise).

During acceleration in the rotating frame of reference, this generates the inertia-type d'Alembert acceleration which drives the liquid toward the trailing face (opposite to rotation direction) at the large radial location of the chamber. Once the flow hits the trailing face, it turns around and the flow is reversed flowing toward the leading face but at the smaller radius. This establishes a clockwise vortex in the R-θ plane. Fig. 4 shows the flow field at t=0.2s as the chamber is rotated counterclockwise with an instantaneous angular speed of 100/s. The tangential velocities are depicted by the two black arrows in Fig. 4.

Coriolis acceleration is induced due to the relative tangential velocity of liquid in the rotating frame. In the mid-plane of the microfluidic chamber (top plane in Fig. 4) the outer tangential velocity, opposite to rotation, induces Coriolis acceleration with fluid moving radially inward (red arrow). Concurrently the inner tangential velocity in the pro-rotation direction induces Coriolis flow radially outward (red arrow). As these two opposite flows meet, the flow is directed axially downward (blue arrow in Fig. 4). As this flow hits the bottom face of the chamber, it gets recirculated upward at the peripheral radial locations, respectively, at R_o and R_i. Thus a pair of counter-rotating vortices or toroidal vortices is being developed due to Coriolis acceleration of the main circulation in the R-θ plane. These vortices provide vertical mixing of momentum and masses, however, the magnitude of velocities are much smaller than the main circulation.

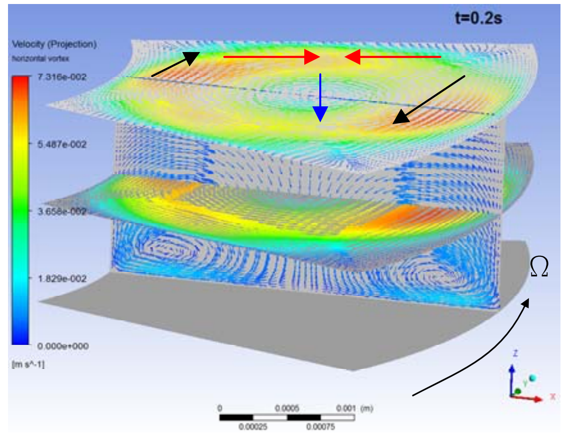

Fig. 4 – Flow field at 0.2 s during acceleration linearly to 250/s over 0.5 s.

During deceleration, all the flow directions reverses compared to Fig. 4 which is for acceleration in the counter-clockwise direction.

When the species in the liquid does not affect the flow (assuming concentration by volume of species less than 2%), we can use the flow field as determined previously to solve the convective-diffusion equation which governs the transport of the species with concentration C.

$$\frac{\partial C}{\partial t} + \nabla \cdot (qC) = \nabla \cdot (D \nabla C) + S \tag{3}$$

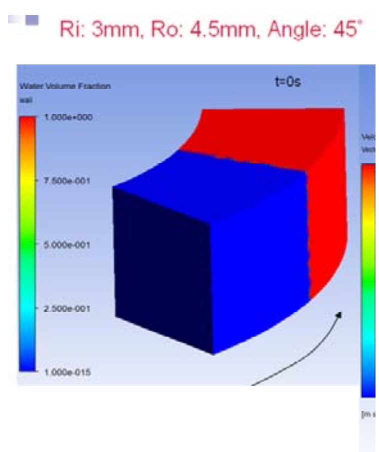

Fig. 5 – Distribution of two colors blue and red initially.

This represents monitoring of the concentration of a given species in time (first term on left side of Eq. 3) and this is affected by convection from main flow (second term of left side of Eq. 3), diffusion from concentration gradient in space (first term of right side of Eq. 3), and source terms, which is absent in this problem. Fig. 5 shows the initial concentration of two species designated as red and blue color, each occupying half of the chamber in the angular sense. Fig. 6 shows the subsequent concentration after 0.1s due to the secondary flow generated (flow direction also represented by arrows in Fig. 6). The contribution of mixing from the primary vortex in the R-θ plane and the double vortices in the R-z plane are clearly seen.

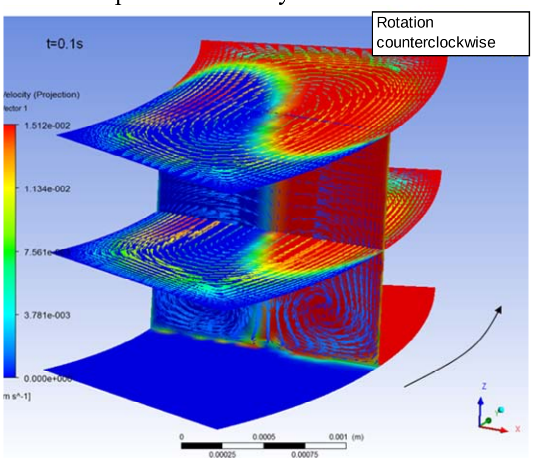

Fig. 6 - Mixing of red and blue color after 0.1 s from rest at t=0 during acceleration in the first cycle.

Mixing can be analyzed by examining the mixing quality which is related to the concentration distribution at any given time. The concentration of species at every point in the chamber is collectively compared to the case when the species is homogeneously mixed in the chamber. This defines the quality factor σ. It corresponds to zero when the species and concentration are distinctly different between regions in the chamber, and when thoroughly mixed in the chamber it corresponds to unity [27]. Given the quality factor approaching unity may take many cycles to accomplish, the curve exhibits a diminishing return behavior. Therefore, the time for complete mixing is arbitrary taken as when σ =90%. Further, we define a specific mixing time SMT as the time for complete (i.e. σ =90%) mixing per unit chamber volume. Small SMT refers to better mixing for a given unit volume of mixture and in contrast large SMT to poorer mixing for unit volume of mixture.

Fig. 7 shows the results expressed as SMT corresponding to two design geometries. The two categories both have inner radius R_i=3 mm while one category has R_o=6 mm and the other with R_o=4.5 mm. Also, both categories have angular span which varies from 22.5° to 45°. It is found that larger R_o with stronger primary circulation and larger volume produces lower SMT. In addition larger angular span has lower SMT. For example, the chamber with 45° is better than the 30° which in turn is better than 22.5°. Larger angular span also implies larger chamber volume. The effect of larger volume (either larger Ro or larger angular span θ) implies more effective secondary flow and circulation as a result of the d'Alembert acceleration during acceleration and deceleration phases, and less viscous resistance from the side, top and bottom walls of the chamber.

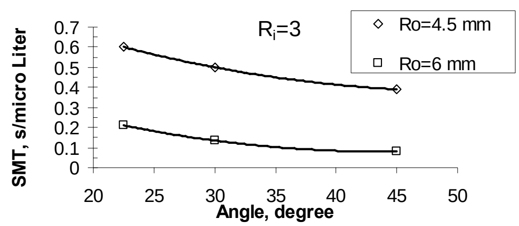

Fig. 7 – Specific mixing time as a function of angular span for two geometries of rotating chamber respectively with R_o=4.5 mm and R_o=6 mm, while both have R_i=3 mm.

Conclusions

A numerical model has been developed on mixing in rotating microfluidics. We found that a primary vortex in the R-θ plane is developed during acceleration of the chamber. Also, a pair of toroidal vortices is developed based on the primary circulation. These pair of vortices is responsible for flow and thus mixing of species in the vertical R-z planes. Several chamber geometries are being studied to produce effective mixing and it was found that the chamber that has larger radius and angular extent provide better mixing per unit volume of liquids to be mixed.

References

[1] Dieter Bothe, Carsten Stemich, Hans-Joachim Warnecke, Computation of scales and quality of mixing in a T-shaped microreactor, Computers and Chemical Engineering 32 (2008) 108–114.
[2] Liu et al. Passive Mixing in a Three Dimensional Serpentine Microchannel. JMEMS, vol. 9, no. 2, June 2000.
[3] Timothy J. Johnson, David Ross, Laurie E. Locasio, Rapid Microfluidic Mixing, Analytical Chemistry 2002, 74, 45-51.
[4] Glasgow and Aubrey, Enhancement of microfluidic mixing using time pulsing. Lab on a Chip 3, 2003 p114-120.
[5] Groisman and Steinberg, Efficient mixing at low Reynolds numbers using polymer additives, Letters to Nature, vol 410, 2001, p905.
[6] McQuain et al., Chaotic Mixer Improves Microarray Hybridization, Analytical Biochemistry, 325, 2004, p215.
[7] Park et al. Rapid three-dimensional passive rotation micromixer using the breakup process. Journal of Micromechanics and Microengineering. 14, 2004, p6-14.
[8] Stroock et al., Chaotic Mixer for Microchannels. Science, 295, 2002, p647.
[9] Drese, Klaus Stefan, Optimization of interdigital micromixers via analytical modeling. Chem. Eng. Journ. 101, 2004, p403-407.
[10] Engler et al. Numerical and Experimental investigations on liquid mixing in static micromixers, Chemical Engineering Journal, 101, 2004, p315-322.
[11] Chamarthy and Wereley, Mixing Characteristics in a serpentine micro-channel. IMECE 2004 (ASME Conference, Anaheim, CA IMECE2004-61902).
[12] M. Grumann, A. Geipel, L. Riegger, R. Zengerle and J. Ducree, Batch-mode mixing on centrifugal microfluidic platforms, Lab Chip, 2005, 5, 560–565.
[13] Grumann, M.; Geipel, A.; Riegger, L.; Zengerle, R.; Ducre′e, J. Batch mode mixing with magnetic beads on centrifugal microfluidic platforms. Lab Chip 2005, 5, 560–565.
[14] Duffy DC, Gills HL, Lin J, Sheppard NF, Kellogg GJ. 1999. Microfabricated centrifugal microfluidic systems: characterization and multiple enzymatic assays. Anal. Chem. 71(20):4669–78.
[15] Madou MJ, Kellogg GJ. 1998. The LabCDTM: a centrifuge-based microfluidic platform for diagnostics. In Systems and Technologies for Clinical Diagnostics and Drug Discovery, ed. GE Cohn, A Katzir, 3259:80–93. San Jose, CA:SPIE.
[16] Ekstrand G, Holmquist C, O¨ rlefors AE, Hellman B, Larsson A, Anderson P. 2000. Microfluidics in a rotating CD. See Ref. 53, pp. 311–14.
[17] Kovacs GTA. 1998. Microfluidic devices. In Micromachined Transducers Sourcebook, Chap. 9, pp. 787–93. Boston:WCB/McGraw-Hill.
[18] Madou MJ. 2002. Fundamentals of Microfabrication. Boca Raton, London, New York,Washington DC: CRC Press. 2nd ed.
[19] Ekstrand G, Holmquist C, O¨ rlefors AE, Hellman B, Larsson A, Anderson P. 2000. Microfluidics in a rotating CD. See Ref. 53, pp. 311–14.
[20] Tiensuu AL, O¨ hman O, Lundbladh L, Larsson O. 2000. Hydrophobic valves by ink-jet printing on plastic CDs with integrated microfluidics. See Ref. 53, pp. 575–78.
[21] Madou MJ, Lu Y, Lai S, Lee J, Daunert S. 2000. A centrifugal microfluidic platform—a comparison. See Ref. 53, pp. 565–70.
[22] Zeng J, Banerjee D, Deshpande M, Gilbert JR, Duffy DC, Kellogg GJ. 2000. Design analysis of capillary burst valves in centrifugal microfluidics. See Ref. 53, pp. 579–82.
[23] Badr IHA, Johnson RD, Madou MJ, Bachas LG. 2002. Fluorescent ion-selective optode membranes incorporated onto a centrifugal microfluidics platform. Anal. Chem. 74(21):5569–75.
[24] Johnson RD, Badr IHA, Barrett G, Lai S, Lu Y, et al. 2001. Development of a fully integrated analysis system for ions based on ion-selective optodes and centrifugal microfluidics. Anal. Chem. 73(16):3940–46
[25] Lynn A Melton, C.W. Lipp, R. W. Spradling, K.A. Paulson, DISMT – Determination of Mixing Time through Color Changes, Engineering Sciences, Fluid Mechanics and Mixing Group Dow Chemical Company, B-1226 Freeport, TX 77541
[26] Leung Wallace WF, Mixing in centrifugal or rotating microfluidics, patent pending, 2008.
[27] Lynn A Melton, C.W. Lipp, R. W. Spradling, K.A. Paulson, DISMT – Determination of Mixing Time through Color Changes, Engineering Sciences, Fluid Mechanics and Mixing Group Dow Chemical Company, B-1226 Freeport, TX 77541.

Acknowledgements
The authors acknowledged the funding support from the Grant Research Council under project GRF/B-Q15S of the research and the postgraduate study of Yong REN at the Hong Kong Polytechnic University.